

# Dalton Transactions

Accepted Manuscript



This article can be cited before page numbers have been issued, to do this please use: D. Van Craen, M. Schlottmann, W. Stahl, C. Räuber and M. Albrecht, *Dalton Trans.*, 2019, DOI: 10.1039/C9DT01065C.



This is an Accepted Manuscript, which has been through the Royal Society of Chemistry peer review process and has been accepted for publication.

Accepted Manuscripts are published online shortly after acceptance, before technical editing, formatting and proof reading. Using this free service, authors can make their results available to the community, in citable form, before we publish the edited article. We will replace this Accepted Manuscript with the edited and formatted Advance Article as soon as it is available.

You can find more information about Accepted Manuscripts in the [author guidelines](#).

Please note that technical editing may introduce minor changes to the text and/or graphics, which may alter content. The journal's standard [Terms & Conditions](#) and the ethical guidelines, outlined in our [author and reviewer resource centre](#), still apply. In no event shall the Royal Society of Chemistry be held responsible for any errors or omissions in this Accepted Manuscript or any consequences arising from the use of any information it contains.

## Kinetic investigation of the dissociation of dinuclear hierarchically assembled titanium(IV) helicates

David Van Craen,<sup>a</sup> Marcel Schlottmann,<sup>a</sup> Wolfgang Stahl,<sup>b</sup> Christoph Rauber,<sup>a</sup> Markus Albrecht<sup>\*a</sup>

Received 00th January 20xx,  
Accepted 00th January 20xx

DOI: 10.1039/x0xx00000x

www.rsc.org/

Hierarchically assembled helicates consisting of lithium-bridged triscatecholate titanium(IV) complexes represent a powerful self-assembled supramolecular system with applications as e.g. molecular balances for the evaluation of weak interactions, stereoselectivity switches in asymmetric synthesis or molecular switch. The respective applications or properties are based on the monomer-dimer equilibrium which easily can be observed in solution. The dimer is the only species in the crystal. After dissolution, the dimer slowly dissociates into the monomer until the equilibrium is reached. This can be followed by NMR spectroscopy to observe the kinetics of the dissociation process. A strong steric effect can be found studying differently substituted ligands. Activation energies of the dissociation process can be correlated with the size of the ester substituents and the system may be described as a molecular buckle.

### Introduction

In 1987 Jean-Marie Lehn defined the term “helicate” for coordination compounds in which two or more ligand strands twist around two or more metal centers.<sup>1</sup> In the following years the chemistry of helicates gained more and more interest as simple models for the understanding of supramolecular key principles like self-assembly.<sup>2,3</sup> Besides the classical “helicate” possessing covalently bridged ligand strands, hierarchically assembled helicate-type systems<sup>4–15</sup> came into focus more than a decade later. A first example of those remarkable supramolecular structures<sup>16</sup> had already been known 25 years before Lehn’s pioneering work on helicates. Hierarchical assembly is based on two (or more) consecutive recognition events: the formation of a Werner-type complex is followed by dimerization<sup>17, 18–21</sup>.

Our group utilizes catechol ligands with aldehyde, ketone or ester substituents in the 3-position for the formation of hierarchically assembled lithium-bridged titanium(IV)<sup>17,22–27</sup>, gallium(III)<sup>17</sup>, boron(III)<sup>28</sup> and molybdenum(VI)dioxo<sup>29</sup> helicate-type complexes. It was shown in the past that the dimer is usually found in the solid state while in solution both monomer and dimer can be easily observed via <sup>1</sup>H NMR spectroscopy.<sup>17,25,26</sup> The dimer stability depends on the strength of the coordination of lithium cations to the salicylate units of two monomers. The crucial role of the solvent<sup>17,23</sup> as

well as the influence of the electron density at the carbonyl group<sup>30</sup> were pointed out earlier. Solvents which can coordinate lithium cations well in solution (e.g. DMSO) destabilize the dimer, while solvents which show a lower affinity (e.g. methanol) result in a higher dimer stability. In a recent study the effect of weak interactions, e.g. solvent as well as dispersive forces between the ester side chains has been addressed. In the earlier study it was realized that the thermodynamic equilibrium in some cases needs some time to be reached.<sup>31</sup> This observation of a “slow” equilibration behaviour in DMSO opens up the way for kinetic investigations of the monomer-dimer equilibrium by NMR spectroscopy and finally allows the determination of activation barriers.

Furthermore, understanding the kinetics of the system cannot be underestimated in order to use the dimerization process at its equilibrated state for the development of molecular devices, like switches.<sup>32</sup>

### Results and discussion

Catecholester ligands are obtained via esterification of the corresponding alcohol with 2,3-dioxosulfinylbenzoyl chloride<sup>33–36</sup> which in situ is readily prepared from 2,3-dihydroxybenzoic acid and thionyl chloride. Formation of titanium(IV) complexes takes place in methanol with the ligands (3 eq.), titanoyl acetylacetonate (1 eq.) and lithium carbonate (1 eq.).

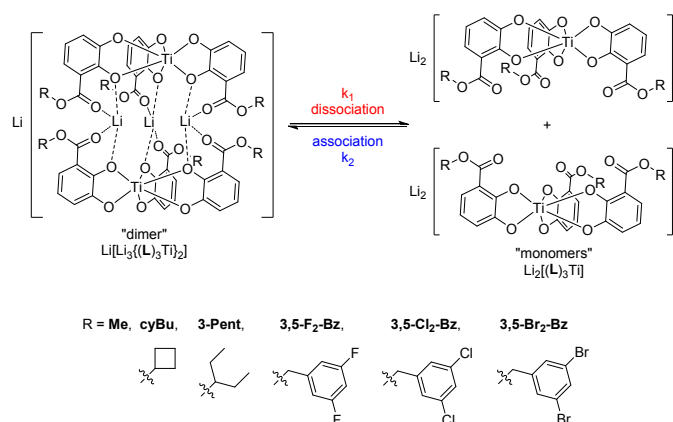
Dissolution of the solid dimeric complexes  $\text{Li}[\text{Li}_3\{(\text{L})_3\text{Ti}\}_2]$  at room temperature in DMSO-*d*<sub>6</sub> at a concentration of  $2.0 \cdot 10^{-3}$  mol L<sup>-1</sup> initially leads to a solution of dimer which slowly dissociates and finally ends up in the thermodynamic ratio between monomer and dimer (scheme 1). In order to obtain energetic parameters for the reaction the disappearance of the dimer and the appearance of the monomer are followed.

<sup>a</sup> Institut fur Organische Chemie, RWTH Aachen University, Landoltweg 1, 52074 Aachen; Germany; markus.albrecht@oc.rwth-aachen.de.

<sup>b</sup> Institut fur Physikalische Chemie, RWTH Aachen University, Landoltweg 2, 52074 Aachen; Germany.

† Electronic Supplementary Information (ESI) available: [NMR spectra, solution of the kinetic equation and kinetic plots]. See DOI: 10.1039/x0xx00000x

To observe a significant change of both dimer and monomer NMR signals, complexes with low dimerization tendency in DMSO- $d_6$  provide the best results, causing a fast initial increase of the monomer signals which is essential to reduce errors based on the signal to noise ratio.



**Scheme 1:** Studied equilibria between hierarchical helicates as dimers and the corresponding triscatecholate complexes as monomers.

The  $^1\text{H}$  NMR spectrum of  $\text{Li}[\text{Li}_3\{(\text{Me})_3\text{Ti}\}_2]$  (figure 1) shows two sets of aromatic signals (doublet of doublets, triplet and doublet of doublets) as well as singlets for each, the dimer (red) and the monomer (blue). The initial spectrum (measured 4 minutes after dissolving the dimer) shows small signals of the monomer.

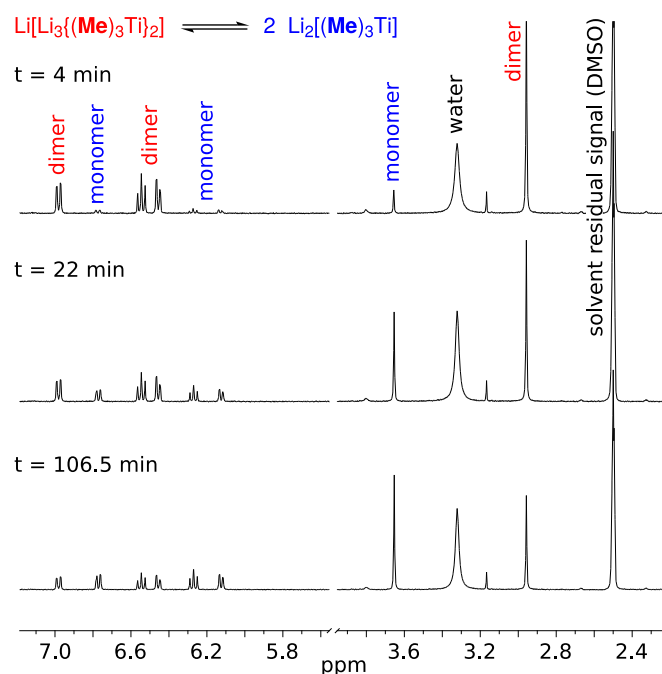


**Figure 1:**  $^1\text{H}$  NMR observation ( $c_0 = 2 \text{ mM}$ ) of the equilibration process. (Regions without signals were removed for clarity reasons - see supporting information for the full spectra)

After 22 minutes the concentration of the monomer already exceeds the one of the dimer (twice the amount equivalent protons is present in the dimeric structure compared to the monomeric one). The equilibrium is reached after 106.5 minutes with a final dimer concentration of  $9.13 \cdot 10^{-4} \text{ mol L}^{-1}$  and a monomer concentration of  $2.17 \cdot 10^{-3} \text{ mol L}^{-1}$ .

Visualizing the dimer  $\text{Li}[\text{Li}_3\{(\text{Me})_3\text{Ti}\}_2]$  concentration (figure 2, top) in dependency to time results in an expected exponential decay of the dimer (red) while the amount of monomer  $\text{Li}_2\{(\text{Me})_3\text{Ti}\}$  (blue) increases.

The other investigated complexes show slower equilibration behaviour in contrast to the methyl substituted complex (figure 2, bottom). The necessary period for reaching the equilibrium is multiple times higher for the cyclobutyl substituted complex  $\text{Li}[\text{Li}_3\{(\text{cyBu})_3\text{Ti}\}_2]$  and drastically increases for the 3-pentyl complex  $\text{Li}[\text{Li}_3\{(\text{3-Pent})_3\text{Ti}\}_2]$ , which is followed for eleven hours (not all data points are shown in figure 2, see SI for the full measurement). At this point the equilibrium state was not even close. The dimerization constant  $K_{\text{dim}}$ , which is necessary for the determination of the rate constants, was measured for  $\text{Li}[\text{Li}_3\{(\text{3-Pent})_3\text{Ti}\}_2]$  after three days.

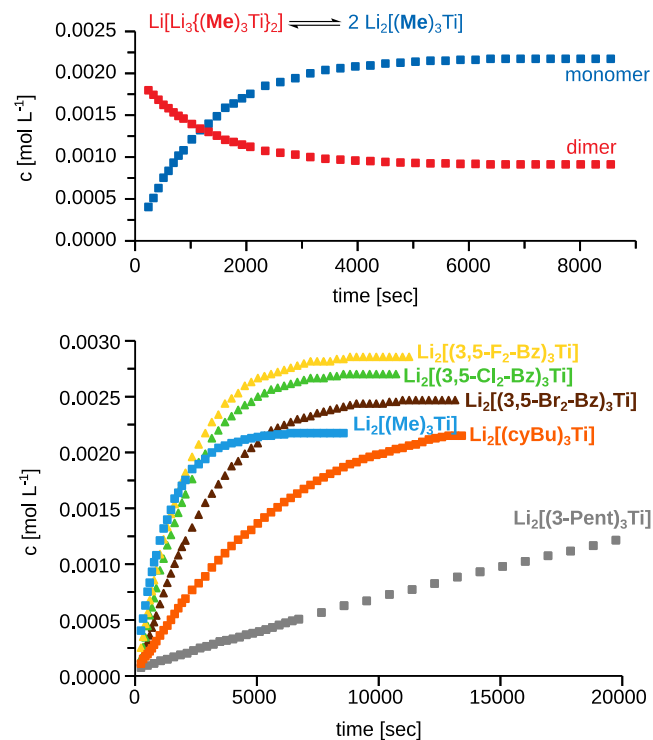


**Figure 2:** Concentration of monomer and dimer of the methyl substituted complex in DMSO- $d_6$  depending on the time after dissolution (top). Comparison of the time dependent increase of monomer concentration of all investigated complexes (bottom).

The complexes with methyl and benzyl esters show a significant faster dissociation behaviour than the cyclobutyl and the 3-pentyl substituted coordination compounds. The halogenated benzyl esters (scheme 1) are investigated to understand the impact of the distance between the sterical demanding residue and the helical cleft. The choice of

halogenated benzyl esters depends also on their low dimer stability which is comparable to the stability of the alkyl ester complexes. The low dimer stability is crucial in order to observe sufficient concentration changes of the monomer and dimer species via NMR spectroscopy and to minimize errors. The difference in between the halogenated benzyl series is not significant and shows that the kinetics depend mainly on steric effects in close proximity of the helical structure or even in the helical cleft. The obtained rate constants provide a more detailed comparison and allow the calculation of the activation energies. The approach to solve the kinetics (see supporting information for mathematic solution) of the reaction leads to a linear equation including the rate constant  $k_2$  as slope.

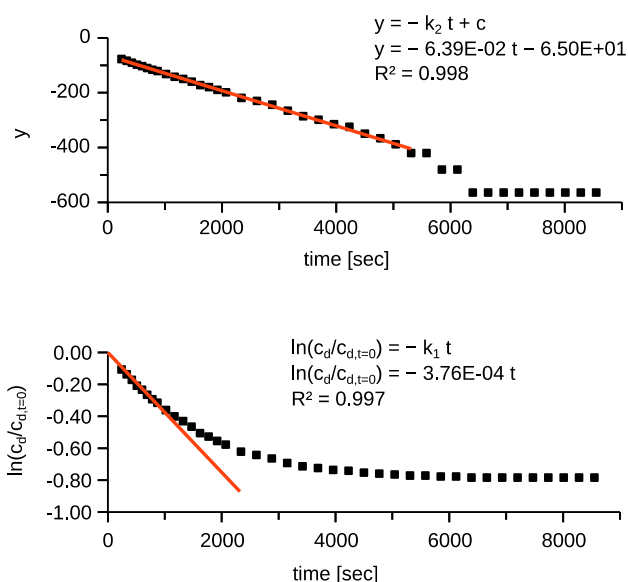
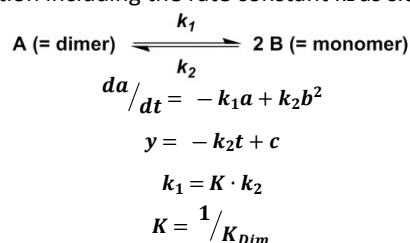


**Figure 3:** Calculation of rate constants by following the kinetic approach (top) and based on the initial slope (bottom).

The kinetics are solved for the dimer dissociation.  $K$  represents the dissociation constant. The rate  $k_1$  can be calculated via  $k_2$  and  $K$ . The final data points close to the equilibrium show a stepwise shape and are excluded in the linear regression to maintain accuracy. The rate constants for the association and dissociation of the methyl complex  $\text{Li}[\text{Li}_3\{(\text{Me})_3\text{Ti}\}_2]$  in  $\text{DMSO}-d_6$  are  $k_2 = 6.39 \cdot 10^{-2} \text{ L mol}^{-1} \text{ s}^{-1}$  and  $k_1 = 3.29 \cdot 10^{-4} \text{ s}^{-1}$ . The rate constant  $k_1$  can also be obtained via the initial slope of  $\ln(C_d/C_{d,t=0})$  as a function of time.<sup>37</sup> At this point  $k_1$  can be estimated according to a first order reaction. The rate constant  $k_1 = 3.76 \cdot 10^{-4} \text{ s}^{-1}$  obtained by this route results in a similar value with a difference of 14 % according to the previous calculated rate constant following the kinetic approach.

The rate constants for all complexes are “mirroring” the behaviour observed in figure 2 bottom. Complexes bearing fluoride, chloride and bromide substituents in the *meta* position of the benzyl ester show very similar rate constants (table 1, entry 4-6). The methyl complex (table 1, entry 1) shows a dissociation rate which is twice as high than the ones of the halogenated benzyl complexes while a lower rate is observed for the cyclobutyl substituted complex (table 1, entry 2). On the other hand the association rate of the methyl substituted monomers is slightly increased in comparison to the halogenated ones while the association of the cyclobutyl bearing monomer units is significantly reduced. The 3-pentyl complex (table 1, entry 3), which bears the most sterically hindered residue of this series, shows drastically reduced dissociation and association rates which are around one order of magnitude lower. The values reveal the strong dependency of the dissociation and association rates on steric effects close to the helical cleft. The benzyl systems including a methylene spacer between the carboxyl function and the bulky aromatic residues are right beyond the methyl complex according to their equilibration behaviour while cyclic and branched systems without a methylene unit show significantly lower rate constants.

**Table 1:** Rate constants determined by following the kinetic approach for the dissociation and association of dimeric hierarchically assembled helicites in  $\text{DMSO}-d_6$  at 25 °C.

entry	substituent	$K_{Dim.}$ [L mol <sup>-1</sup> ]	dissociation rate $k_2$ [L mol <sup>-1</sup> s <sup>-1</sup> ]	association rate $k_1$ [s <sup>-1</sup> ]
1	<b>Me</b>	194 ± 20	6.39 · 10 <sup>-2</sup> ± 0.90 · 10 <sup>-2</sup>	3.29 · 10 <sup>-4</sup> ± 0.46 · 10 <sup>-4</sup>
2	<b>cyBu</b>	174 ± 18	1.74 · 10 <sup>-2</sup> ± 0.09 · 10 <sup>-2</sup>	9.99 · 10 <sup>-5</sup> ± 0.49 · 10 <sup>-5</sup>
3	<b>3-Pent</b>	57 ± 6	1.03 · 10 <sup>-3</sup> ± 0.03 · 10 <sup>-3</sup>	1.80 · 10 <sup>-5</sup> ± 0.04 · 10 <sup>-5</sup>
4	<b>3,5-F<sub>2</sub>-Bz</b>	70 ± 7	2.24 · 10 <sup>-2</sup> ± 0.09 · 10 <sup>-2</sup>	3.20 · 10 <sup>-4</sup> ± 0.13 · 10 <sup>-4</sup>
5	<b>3,5-Cl<sub>2</sub>-Bz</b>	89 ± 9	2.70 · 10 <sup>-2</sup> ± 0.51 · 10 <sup>-2</sup>	3.04 · 10 <sup>-4</sup> ± 0.58 · 10 <sup>-4</sup>
6	<b>3,5-Br<sub>2</sub>-Bz</b>	126 ± 13	2.64 · 10 <sup>-2</sup> ± 0.57 · 10 <sup>-2</sup>	2.10 · 10 <sup>-4</sup> ± 0.45 · 10 <sup>-4</sup>

Dispersive forces may occur between the ester residues of two dimer halves<sup>31</sup>. Dispersion is negligible for the methyl and cyclobutyl complex due to the long CH-CH distances between the ester residues as shown already in earlier studies.<sup>31</sup> Thus, steric demand is the main reason for the different kinetic behaviour and the system can be described as a molecular symmetric buckle. The size of the “teeth” of the buckle halves reflects the steric demand of the ester residue. The activation energies for the association and dissociation of the methyl and cyclobutyl substituted complexes are shown as exemplary systems to illustrate this model. The equilibration

behaviour therefore was monitored at five different temperatures (figure 4). Starting from 25 °C the temperature was increased in steps of 10 °C up to 65 °C.

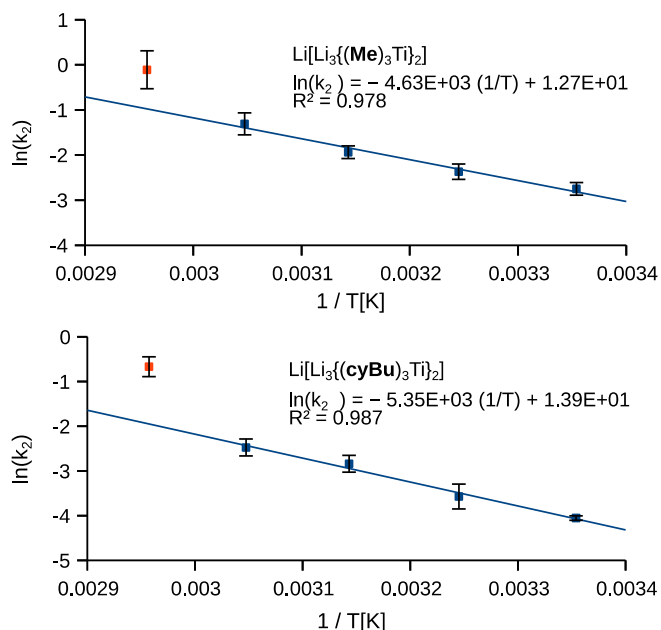


**Figure 4:** Calculation of activation energies of the dimer association for the methyl (top) and cyclobutyl substituted complex (bottom). The red values obtained at 65 °C are excluded in the linear regression analysis.

activation energy of the dimerization going from the methyl to the cyclobutyl derivative. More energy is needed in order to lock the bigger groups in the dimer or to disrupt the dimer to form the monomers.

Thus, the system mimics a symmetric molecular buckle. Closing the lock with bigger “teeth” (increased steric demand) takes more strength to push the halves together as well as to open the lock.

## Conclusions

Herein we investigated the kinetics of the formation of hierarchically assembled lithium-bridged titanium(IV) helicates (dimer) as well as their dissociation to the corresponding “Werner” type triscatecholate complexes (monomer). The kinetic behaviour shows that the underlying processes in this system behave like a molecular buckle. With bigger side groups the necessary energy for closing and opening the lock increases, resulting in lower reaction rates.

Understanding the kinetics of this system changes our perspective for so far more challenging systems bearing extreme bulky ester substituents. Thus, investigating the limit of the steric demand of the substituents is required for the design of future functional materials.

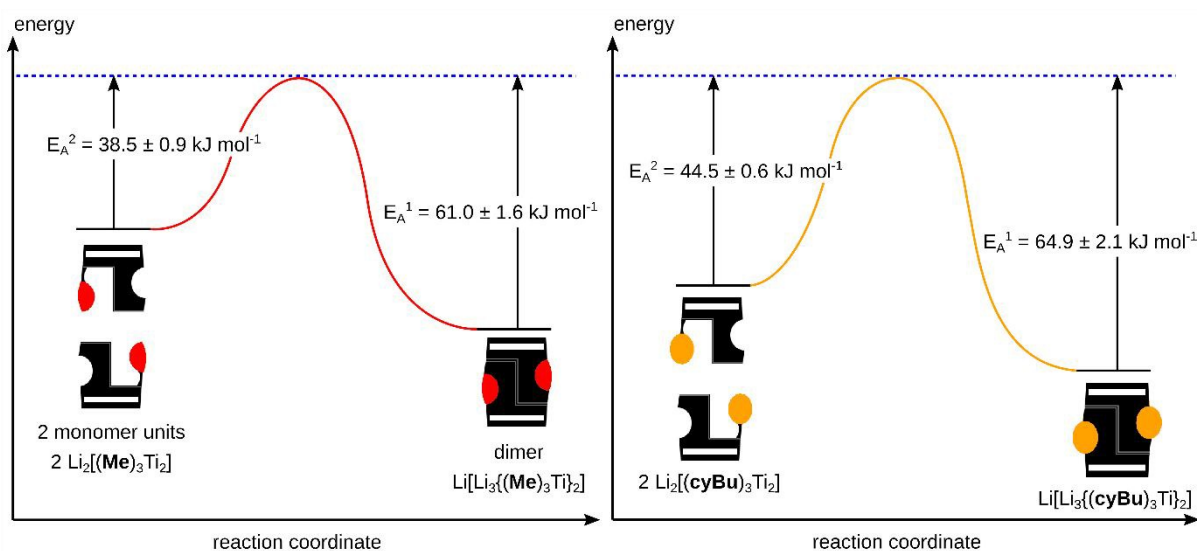


**Figure 5:** Visualization of the symmetric molecular snap lock with the methyl (left) and the cyclobutyl complex (right).

The rate constant at 65°C represents an aberration due to the rapid equilibration coming along with too less values for an accurate calculation of the rate constants by linear regression. It is excluded in both cases.

Energies of activation are obtained with the assumption of a nearly temperature independent Arrhenius factor. The values (figure 5) reflect the behaviour of the rate constants for the methyl  $\text{Li}[\text{Li}_3\{(\text{Me})_3\text{Ti}\}_2]$  and the cyclobutyl complex  $\text{Li}[\text{Li}_3\{(\text{cyBu})_3\text{Ti}\}_2]$ . An increase of 6  $\text{kJ mol}^{-1}$  is observed for the

## Experimental

### Materials and methods:

2,3-Dihydroxybenzoic acid was purchased from FluoroChem, thionyl chloride from Acros and the corresponding alcohols from Alfa Aesar, abcr GmbH and TCI. All chemicals were used without further purification. The used  $\text{DMSO-}d_6$  (99.9 %, with 0.05 % TMS as

internal standard) was procured from Cambridge Isotope Laboratories. NMR spectroscopy was carried out on a Mercury 300 as well as a Varian NMR 400 and 600 device. Mass spectrometry was measured using a LTQ Orbitrap XL device. IR spectra were obtained with a Perkin-Elmer Spektrum 100 spectrometer. Elemental composition was detected with a Heraeus CHN-O-Rapid device.

#### General method for ligand synthesis:

2,3-Dihydroxybenzoic acid (1 eq.) was heated under reflux conditions in thionyl chloride (30 eq.) for three hours. Full conversion was observed (transition from a suspension to clear solution). After this time remaining thionyl chloride was removed under reduced pressure. The obtained 2,3-dioxosulfinylbenzoyl chloride was not further purified and diluted with chloroform. A solution of the corresponding alcohol (5 eq.) and triethylamine (5 eq.) in chloroform was added to the solution of the 2,3-dioxosulfinylbenzoyl chloride in chloroform, resulting in a 0.2 molar solution. The mixture was heated under reflux conditions for 24 hours. Afterwards the reaction mixture was washed with saturated NaHCO<sub>3</sub> solution and dried over MgSO<sub>4</sub>. The desired product was isolated and purified by column chromatography with silica gel 60 (35 – 70 μm).

#### General method for helicate synthesis:

Catechol ligand (3 eq.), TiO(acac)<sub>2</sub> (1 eq.) and Li<sub>2</sub>CO<sub>3</sub> (1 eq.) were dissolved in MeOH (0.02 M) and stirred for 24 hours. Afterwards, the solvent was removed under reduced pressure and the desired complex was received as a red solid without further purification.

**Literature known compounds:** Catechol ligands **Me-H<sub>2</sub>**<sup>17</sup>, **cyBu-H<sub>2</sub>**<sup>31</sup> and **3-Pent-H<sub>2</sub>**<sup>31</sup> as well as their corresponding titanium complexes Li[Li<sub>3</sub>{(Me)<sub>3</sub>Ti<sub>2</sub>}]<sup>17</sup>, Li[Li<sub>3</sub>{(cyBu)<sub>3</sub>Ti<sub>2</sub>}]<sup>31</sup> and Li[Li<sub>3</sub>{(3-Pent)<sub>3</sub>Ti<sub>2</sub>}]<sup>31</sup> are well described in the literature.

#### 3,5-Difluorobenzyl-2,3-dihydroxybenzoate ((3,5-F<sub>2</sub>-Bz)-H<sub>2</sub>):

Yield = 45 % (810 mg, 2.89 mmol, colourless solid). M.p. = 98 °C. <sup>1</sup>H NMR (400 MHz, CDCl<sub>3</sub>, 25 °C): δ = 10.71 (s, 1H, OH), 7.42 (dd, *J* = 8.1, 1.5 Hz, 1H, H<sub>arom.</sub>), 7.16-7.12 (m, 1H, H<sub>arom.</sub>), 7.00-6.93 (m, 2H, H<sub>arom.</sub>), 6.86-6.77 (m, 2H, H<sub>arom.</sub>), 5.64 (s, 1H, OH), 5.35 (s, 2H, OCH<sub>2</sub>) ppm. <sup>13</sup>C NMR (101 MHz, CDCl<sub>3</sub>, 25 °C): δ = 169.8 (CO<sub>2</sub>CH<sub>2</sub>), 163.1 (C<sub>arom.</sub>), 149.0 (C<sub>arom.</sub>), 145.1 (C<sub>arom.</sub>), 138.9 (C<sub>arom.</sub>), 120.5 (C<sub>arom.</sub>), 120.2 (C<sub>arom.</sub>), 119.4 (C<sub>arom.</sub>), 111.9 (C<sub>arom.</sub>), 110.6 (C<sub>arom.</sub>), 103.9 (C<sub>arom.</sub>), 65.5 (CO<sub>2</sub>CH<sub>2</sub>) ppm. <sup>19</sup>F NMR (376 MHz, CDCl<sub>3</sub>, 25 °C): δ = -108.9 (t, *J* = 7.6 Hz) ppm. MS (negative ESI-FTMS, MeOH): *m/z* (%) = 279.0495 (95, [M-H<sup>+</sup>], C<sub>14</sub>H<sub>9</sub>F<sub>2</sub>O<sub>4</sub><sup>-</sup>, calc.: 279.0474). IR (in KBr):  $\tilde{\nu}$  (cm<sup>-1</sup>) = 3434 (w), 3214 (w), 2939 (w), 1682 (vs), 1629 (m), 1596 (s), 1469 (s), 1389 (m), 1298 (s), 1255 (s), 1150 (s), 1116 (s), 1072 (m), 1033 (w), 989 (m), 961 (s), 844 (s), 748 (s), 694 (s). Elemental analysis C<sub>14</sub>H<sub>10</sub>F<sub>2</sub>O<sub>4</sub>: calc. C = 60.01 %, H = 3.60 %; found C = 59.92 %, H = 3.67 %.

#### 3,5-Dichlorobenzyl-2,3-dihydroxybenzoate ((3,5-Cl<sub>2</sub>-Bz)-H<sub>2</sub>):

Yield = 35 % (716.8 mg, 2.29 mmol, colourless solid). M.p. = 103 °C. <sup>1</sup>H NMR (400 MHz, CDCl<sub>3</sub>, 25 °C): δ = 10.70 (s, 1H, OH), 7.41 (dd, *J* = 8.1, 1.5 Hz, 1H, H<sub>arom.</sub>), 7.36 (t, *J* = 1.8 Hz, 1H, H<sub>arom.</sub>), 7.32 (d, *J* = 1.8 Hz, 2H, H<sub>arom.</sub>), 7.17-7.09 (m, 1H, H<sub>arom.</sub>), 6.83 (t, *J* = 8.0 Hz, 1H,

H<sub>arom.</sub>), 5.65 (s, 1H, OH), 5.32 (s, 2H, OCH<sub>2</sub>) ppm. <sup>13</sup>C NMR (151 MHz, CDCl<sub>3</sub>, 25 °C): δ = 169.9 (CO<sub>2</sub>CH<sub>2</sub>), 149.2 (C<sub>arom.</sub>), 145.2 (C<sub>arom.</sub>), 138.6 (C<sub>arom.</sub>), 135.5 (C<sub>arom.</sub>), 128.9 (C<sub>arom.</sub>), 126.6 (C<sub>arom.</sub>), 120.7 (C<sub>arom.</sub>), 120.4 (C<sub>arom.</sub>), 119.6 (C<sub>arom.</sub>), 112.1 (C<sub>arom.</sub>), 65.5 (CO<sub>2</sub>CH<sub>2</sub>) ppm. MS (negative ESI-FTMS, MeOH): *m/z* (%) = 310.9881 (50, [M-H<sup>+</sup>], C<sub>14</sub>H<sub>9</sub>Cl<sub>2</sub>O<sub>4</sub><sup>-</sup>, calc.: 310.9883). IR (in KBr):  $\tilde{\nu}$  (cm<sup>-1</sup>): 3443 (m), 3239 (m), 3086 (w), 1677 (s), 1598 (m), 1571 (m), 1467 (s), 1375 (s), 1306 (vs), 1237 (s), 1144 (s), 1067 (m), 1015 (m), 920 (m), 843 (s), 799 (s), 736 (s). Elemental analysis C<sub>14</sub>H<sub>10</sub>Cl<sub>2</sub>O<sub>4</sub>: calc. C = 53.70 %, H = 3.22 %; found C = 53.68 %, H = 3.21 %.

#### 3,5-Dibromobenzyl-2,3-dihydroxybenzoate ((3,5-Br<sub>2</sub>-Bz)-H<sub>2</sub>):

Yield: 69 % (418.0 mg, 1.04 mmol, colourless solid). M.p. = 114 °C. <sup>1</sup>H NMR (300 MHz, CDCl<sub>3</sub>, 25 °C): δ = 10.70 (s, 1H, OH), 7.67 (t, *J* = 1.7 Hz, 1H, H<sub>arom.</sub>), 7.52 (d, *J* = 1.7 Hz, 2H, H<sub>arom.</sub>), 7.41 (dd, *J* = 8.0, 1.5 Hz, 1H, H<sub>arom.</sub>), 7.17-7.09 (m, 1H, H<sub>arom.</sub>), 6.83 (t, *J* = 8.0 Hz, 1H, H<sub>arom.</sub>), 5.64 (s, 1H, OH), 5.31 (s, 2H, OCH<sub>2</sub>) ppm. <sup>13</sup>C NMR (151 MHz, CDCl<sub>3</sub>, 25 °C): δ = 169.9 (CO<sub>2</sub>CH<sub>2</sub>), 149.2 (C<sub>arom.</sub>), 145.2 (C<sub>arom.</sub>), 139.1 (C<sub>arom.</sub>), 134.4 (C<sub>arom.</sub>), 130.0 (C<sub>arom.</sub>), 123.4 (C<sub>arom.</sub>), 120.7 (C<sub>arom.</sub>), 120.4 (C<sub>arom.</sub>), 119.6 (C<sub>arom.</sub>), 112.1 (C<sub>arom.</sub>), 65.4 (CO<sub>2</sub>CH<sub>2</sub>) ppm. MS (negative ESI-FTMS, MeOH, acidified): *m/z* (%) = 400.8859 (100, [M-H<sup>+</sup>], C<sub>14</sub>H<sub>9</sub>Br<sub>2</sub>O<sub>4</sub><sup>-</sup>, calc.: 400.8853). IR (in KBr):  $\tilde{\nu}$  (cm<sup>-1</sup>) = 3510 (m), 3404 (m), 3070 (w), 1668 (s), 1557 (m), 1467 (s), 1381 (m), 1303 (vs), 1139 (vs), 1070 (m), 991 (m), 846 (s), 744 (vs). Elemental analysis C<sub>14</sub>H<sub>10</sub>Br<sub>2</sub>O<sub>4</sub>: calc. C = 41.83 %, H = 2.51 %; found C = 41.81 %, H = 2.67 %.

#### Li[Li<sub>3</sub>{(3,5-F<sub>2</sub>-Bz)<sub>3</sub>Ti<sub>2</sub>}]:

Yield: quantitative (140 mg, 78 μmol, red solid). <sup>1</sup>H NMR (400 MHz, DMSO-*d*<sub>6</sub>, 25 °C): Monomer (major component): δ = 6.83 (dd, *J* = 7.8, 1.5 Hz, 1H, H<sub>arom.</sub>), 6.29 (t, *J* = 7.8 Hz, 1H, H<sub>arom.</sub>), 6.17 (dd, *J* = 7.8, 1.5 Hz, 1H, H<sub>arom.</sub>), 5.19 (s, 2H, OCH<sub>2</sub>) ppm. Dimer (minor component): δ = 7.03 (dd, *J* = 7.9, 1.4 Hz, 1H, H<sub>arom.</sub>), 6.96-6.88 (m, 2H, H<sub>arom.</sub>), 6.54 (dd, *J* = 7.9, 1.4 Hz, 1H, H<sub>arom.</sub>), 6.38 (t, *J* = 7.9 Hz, 1H, H<sub>arom.</sub>), 4.63 (d, *J* = 13.7 Hz, 1H, OCH<sub>2</sub>), 3.98 (d, *J* = 13.7 Hz, 1H, OCH<sub>2</sub>) ppm. The other benzyl ester signals are overlapping and are not assigned. MS (negative ESI-FTMS, MeOH): *m/z* (%) = 1785.1838 (100, [M-Li<sup>+</sup>], C<sub>84</sub>H<sub>48</sub>F<sub>12</sub>O<sub>24</sub>Li<sub>3</sub>Ti<sub>2</sub><sup>-</sup>, calc.: 1785.1788). IR (in KBr):  $\tilde{\nu}$  (cm<sup>-1</sup>) = 3372 (w), 1677 (s), 1597 (s), 1443 (s), 1384 (m), 1209 (s), 1065 (m), 946 (s), 844 (s), 744 (s). Elemental analysis C<sub>84</sub>H<sub>48</sub>F<sub>12</sub>O<sub>24</sub>Li<sub>4</sub>Ti<sub>2</sub> × 3 H<sub>2</sub>O: calc. C = 54.63 %, H = 2.95 %; found C = 54.42 %, H = 3.02 %.

#### Li[Li<sub>3</sub>{(3,5-Cl<sub>2</sub>-Bz)<sub>3</sub>Ti<sub>2</sub>}]:

Yield: quantitative (136 mg, 68 μmol, red solid). <sup>1</sup>H NMR (400 MHz, DMSO-*d*<sub>6</sub>, 25 °C): Monomer (major component): δ = 7.44 (d, *J* = 1.5 Hz, 2H, H<sub>arom.</sub>), 6.81 (dd, *J* = 7.8, 1.5 Hz, 1H, H<sub>arom.</sub>), 6.29 (t, *J* = 7.8 Hz, 1H, H<sub>arom.</sub>), 6.16 (dd, *J* = 7.8, 1.5 Hz, 1H, H<sub>arom.</sub>), 5.18 (s, 2H, OCH<sub>2</sub>) ppm. Dimer (minor component): δ = 7.25 (d, *J* = 1.8 Hz, 2H, H<sub>arom.</sub>), 7.02 (dd, *J* = 7.8, 1.4 Hz, 1H, H<sub>arom.</sub>), 6.54 (dd, *J* = 7.8, 1.5 Hz, 1H, H<sub>arom.</sub>), 6.39 (t, *J* = 7.8 Hz, 1H, H<sub>arom.</sub>), 4.59 (d, *J* = 13.5 Hz, 1H, OCH<sub>2</sub>), 3.99 (d, *J* = 13.5 Hz, 1H, OCH<sub>2</sub>) ppm. The not assigned benzyl ester signal is overlapping. MS (negative ESI-FTMS, MeOH): *m/z* (%) = 1982.8169 (100, [M-Li<sup>+</sup>], C<sub>84</sub>H<sub>48</sub>Cl<sub>12</sub>O<sub>24</sub>Li<sub>3</sub>Ti<sub>2</sub><sup>-</sup>, calc.: 1982.8154). IR (in KBr):  $\tilde{\nu}$  (cm<sup>-1</sup>) = 3366 (w), 1678 (s), 1569 (s), 1440 (s), 1374 (m), 1251 (s), 1151 (s), 1011 (s), 921 (m), 849 (s), 797 (s), 681 (s). Elemental analysis C<sub>84</sub>H<sub>48</sub>Cl<sub>12</sub>O<sub>24</sub>Li<sub>4</sub>Ti<sub>2</sub> × 5 H<sub>2</sub>O: calc. C = 48.50 %, H = 2.81 %; found C = 48.54 %, H = 2.71 %.

**Li[Li<sub>3</sub>{(3,5-Br<sub>2</sub>-Bz)<sub>3</sub>Ti]<sub>2</sub>]:**

Yield: quantitative (128 mg, 51 μmol, red solid). <sup>1</sup>H NMR (400 MHz, DMSO-*d*<sub>6</sub>, 25 °C): Monomer (major component): δ = 7.61 (d, *J* = 1.1 Hz, 2H, H<sub>arom.</sub>), 6.81 (dd, *J* = 7.8, 1.2 Hz, 1H, H<sub>arom.</sub>), 6.29 (t, *J* = 7.8 Hz, 1H, H<sub>arom.</sub>), 6.16 (dd, *J* = 7.8, 1.2 Hz, 1H, H<sub>arom.</sub>), 5.17 (s, 2H, OCH<sub>2</sub>) ppm. Dimer (minor component): δ = 7.42 (d, *J* = 1.1 Hz, 2H, H<sub>arom.</sub>), 7.05–6.99 (m, 1H, H<sub>arom.</sub>), 6.57–6.51 (m, 1H, H<sub>arom.</sub>), 6.40 (t, *J* = 7.8 Hz, 1H, H<sub>arom.</sub>), 4.57 (d, *J* = 13.7 Hz, 1H, OCH<sub>2</sub>), 3.98 (d, *J* = 13.7 Hz, 1H, OCH<sub>2</sub>) ppm. The other signal from the benzyl ester residue is overlapping and cannot be assigned. MS (negative ESI-FMST, MeOH): *m/z* (%) = 2516.1992 (100, [M-Li<sup>+</sup>], C<sub>84</sub>H<sub>48</sub>Br<sub>12</sub>O<sub>24</sub>Li<sub>3</sub>Ti<sub>2</sub><sup>-</sup>, calc.: 2516.2054). IR (in KBr):  $\tilde{\nu}$  (cm<sup>-1</sup>) = 3365 (w), 2070 (w), 1678 (s), 1556 (m), 1441 (s), 1209 (s), 1009 (s), 907 (w), 848 (m), 742 (s), 681 (s). Elemental analysis C<sub>84</sub>H<sub>48</sub>Br<sub>12</sub>O<sub>24</sub>Li<sub>3</sub>Ti<sub>2</sub> × 4 H<sub>2</sub>O: calc. C = 38.87 %, H = 2.17 %; found C = 38.88 %, H = 2.29 %.

**Conflicts of interest**

“There are no conflicts to declare”

**Acknowledgements**

We gratefully thank the international research training group SeleCa (Selectivity in Chemo- and Biocatalysis) of the DFG for support.

**References**

- J. M. Lehn, A. Rigault, J. Siegel, J. Harrowfield, B. Chevrier and D. Moras, *Proc. Natl. Acad. Sci. U. S. A.*, 1987, **84**, 2565–9.
- Reviews: (a) C. Piguet, G. Bernardinelli and G. Hopfgartner, *Chem. Rev.*, 1997, **97**, 2005–2062; (b) M. Albrecht, *Chem. Rev.*, 2001, **101**, 3457–3498; (c) E. Yashima, N. Ousaka, D. Taura, K. Shimomura, T. Ikai, and K. Maeda, *Chem. Rev.* 2016, **116**, 13752–13990.
- Recent highlights in helicate chemistry: (a) B. Song, C. D. B. Vandevyver, A.-S. Chauvin, and J.-C. G. Bünzli *Org. Biomol. Chem.*, 2008, **6**, 4125; (b) A. D. Faulkner, R. A. Kaner, Q. M. A. Abdallah, G. Clarkson, D. J. Fox, P. Gurnani, S. E. Howson, R. M. Phillips, D. I. Roper, D. H. Simpson, and P. Scott, *Nature Chem.* 2014, **6**, 797; (c) E. Chinnaraja, R. Arunachalam, E. Suresh, S. K. Sen, R. Natarajan, and P. S. Subramanian, *Inorg. Chem.* 2019, **58**, 4465–4479; (d) Y. Zhang, B. Ali, J. Wu, M. Guo, Y. Yu, Z. Liu, and J. Tang, *Inorg. Chem.* 2019, **58**, 3167–3174; (e) J.-F. Ayme, J. E. Beves, C. J. Campbell, and D. A. Leigh, *J. Am. Chem. Soc.* 2019, **141**, 3605–3612.
- T. Konno, K. Tokuda, T. Suzuki and K. Okamoto, *Bull. Chem. Soc. Jpn.*, 1998, **71**, 1049–1054.
- A. K. Das, A. Rueda, L. R. Falvello, S.-M. Peng and S. Bhattacharya, *Inorg. Chem.*, 1999, **38**, 4365–4368.
- X. Sun, D. W. Johnson, D. L. Caulder, R. E. Powers, K. N. Raymond and E. H. Wong, *Angew. Chem. Int. Ed.*, 1999, **38**, 1303–1307.
- M. Albrecht, K. Witt, H. Röttele and R. Fröhlich, *Chem. Commun.*, 2001, 1330–1331.
- X. Sun, D. W. Johnson, K. N. Raymond and E. H. Wong, *Inorg. Chem.*, 2001, **40**, 4504–4506.
- X. Sun, D. W. Johnson, D. L. Caulder, K. N. Raymond and E. H. Wong, *J. Am. Chem. Soc.*, 2001, **123**, 2752–2763.
- J. Hamblin, L. J. Childs, N. W. Alcock and M. J. Hannon, *J. Chem. Soc. Dalton Trans.*, 2002, **46**, 164–169.
- M. Albrecht, K. Witt, P. Weis, E. Wegelius and R. Fröhlich, *Inorganica Chim. Acta*, 2002, **341**, 25–32. DOI: 10.1039/C9DT01065C
- J. Heinicke, N. Peulecke, K. Karaghiosoff and P. Mayer, *Inorg. Chem.*, 2005, **44**, 2137–2139.
- S. Hiraoka, Y. Sakata and M. Shionoya, *J. Am. Chem. Soc.*, 2008, **130**, 10058–10059.
- Y. Sakata, S. Hiraoka and M. Shionoya, *Chem. - Eur. J.*, 2010, **16**, 3318–3325.
- G. Bauer, Z. Benkő, J. Nuss, M. Nieger and D. Gudat, *Chem. - Eur. J.*, 2010, **16**, 12091–12095.
- D. H. Busch and D. C. Jicha, *Inorg. Chem.*, 1962, **1**, 884–887.
- M. Albrecht, S. Mirtschin, M. de Groot, I. Janser, J. Runsink, G. Raabe, M. Kogej, C. A. Schalley and R. Fröhlich, *J. Am. Chem. Soc.*, 2005, **127**, 10371–10387.
- K. Yoneda, K. Adachi, K. Nishio, M. Yamasaki, A. Fuyuhiko, M. Katada, S. Kaizaki and S. Kawata, *Angew. Chem. Int. Ed.*, 2006, **45**, 5459–5461.
- A.-X. Zhu, J.-P. Zhang, Y.-Y. Lin and X.-M. Chen, *Inorg. Chem.*, 2008, **47**, 7389–7395.
- G. N. Newton, T. Onuki, T. Shiga, M. Noguchi, T. Matsumoto, J. S. Mathieson, M. Nihei, M. Nakano, L. Cronin and H. Oshio, *Angew. Chem. Int. Ed.*, 2011, **50**, 4844–4848.
- M. Okamura, M. Kondo, R. Kuga, Y. Kurashige, T. Yanai, S. Hayami, V. K. K. Praneeth, M. Yoshida, K. Yoneda, S. Kawata and S. Masaoka, *Nature*, 2016, **530**, 465–468.
- M. Albrecht, M. Baumert, H. D. F. Winkler, C. A. Schalley and R. Fröhlich, *Dalton Trans.*, 2010, **39**, 7220–2.
- M. Baumert, M. Albrecht, H. D. F. Winkler and C. A. Schalley, *Synthesis*, 2010, **2010**, 953–958.
- M. Albrecht, E. Isaak, M. Baumert, V. Gossen, G. Raabe and R. Fröhlich, *Angew. Chem. Int. Ed.*, 2011, **50**, 2850–2853.
- M. Albrecht, E. Isaak, V. Moha, G. Raabe and R. Fröhlich, *Chem. - Eur. J.*, 2014, **20**, 6650–8.
- M. Albrecht, E. Isaak, H. Shigemitsu, V. Moha, G. Raabe and R. Fröhlich, *Dalton Trans.*, 2014, **43**, 14636–14643.
- D. Van Craen, M. Albrecht, G. Raabe, F. Pan and K. Rissanen, *Chem. - Eur. J.*, 2016, **22**, 3255–3258.
- M. Albrecht, M. Fiege, M. Baumert, M. De Groot, R. Fröhlich, L. Russo and K. Rissanen, *Eur. J. Inorg. Chem.*, 2007, 609–616.
- M. Albrecht, M. Baumert, J. Klankermayer, M. Kogej, C. A. Schalley and R. Fröhlich, *Dalton Trans.*, 2006, 4395–400.
- D. Van Craen, M. de Groot, M. Albrecht, F. Pan and K. Rissanen, *Z. Anorg. Allg. Chem.*, 2015, **641**, 2222–2227.
- D. Van Craen, W. H. Rath, M. Huth, L. Kemp, C. Räuber, J. M. Wollschläger, C. A. Schalley, A. Valkonen, K. Rissanen and M. Albrecht, *J. Am. Chem. Soc.*, 2017, **139**, 16959–16966.
- (a) X. Chen, T. M. Gerger, C. Räuber, G. Raabe, C. Göb, I. M. Oppel and M. Albrecht, *Angew. Chem. Int. Ed.*, 2018, **57**, 11817–11820. See for comparison: (b) M. Albrecht, X. Chen, D. VanCraen, *Chem. Eur. J.* 2019, **25**, 4265–4273; (c) X. Chen, M. Baumert, R. Fröhlich, M. Albrecht, *J. Incl. Phen. Macrocycl. Chem.* 2019, DOI: 10.1007/s10847-019-00888-9; (d) Y. Suzuki, T. Nakamura, H. Iida, N. Ousaka, and E. Yashima, *J. Am. Chem. Soc.* 2016, **138**, 4852–4859; (e) N. Ousaka, K. Shimizu, Y. Suzuki, T. Iwata, M. Itakura, D. Taura, H. Iida, Y. Furusho, T. Mori, and E. Yashima, *J. Am. Chem. Soc.* 2018, **140**, 17027–17039;
- E. J. Corey and S. Bhattacharyya, *Tetrahedron Lett.*, 1977, **18**, 3919–3922.
- E. J. Corey and S. D. Hurt, *Tetrahedron Lett.*, 1977, **18**, 3923–3924.
- F. L. Weigl and K. N. Raymond, *J. Am. Chem. Soc.*, 1979, **101**, 2728–2731.

## Journal Name

## ARTICLE

- 36 C. J. Gramer and K. N. Raymond, *Org. Lett.*, 2001, **3**, 2827–2830.
- 37 K. J. Hall, T. I. Quickenden and D. W. Watts, *J. Chem. Educ.*, 1976, **53**, 493–493.

View Article Online  
DOI: 10.1039/C9DT01065C

Dalton Transactions Accepted Manuscript

